Fifth International Symposium on Cavitation (CAV2003)
Osaka, Japan,November 1-4, 2003

NUMERICAL ANALYSIS FOR UNSTEADY CVITATING FLOW IN A PUMP INDUCER

Kohei OKITA
Intelligent Modeling Laboratory,
The University of Tokyo
2-11-16 Yayoi, Bunkyo,
Tokyo 113-8656, Japan
Email: okita@fel.t.u-tokyo.ac.jp

Yoichiro MATSUMOTO
Department of Mechanical Engineering,
The University of Tokyo
7-3-1 Hongo, Bunkyo,
Tokyo 113-8656, Japan
Email: ymats@mech.t.u-tokyo.ac.jp

Kenjiro KAMIJO
Institute of Fluid Science,
Tohoku University
2-1-1 Katahira, Aoba, Sendai,
Miyagi 980-0812, Japan
Email: kamijyo@ifs.tohoku.ac.jp

ABSTRACT

In cavitating flows of turbomachines, instabilities as the cavitation surge and the rotating cavitation are observed. The objective of the present study is to reproduce these unstable phenomena in cavitating flows by numerical simulation. Our method is based on the numerical method for incompressible fluid flow, but which has been employed the compressibility through the low Mach number as an assumption. The evolution of cavitation is determined by an existing cavitation model with some modification that is represented by the source/sink of vapor phase in the liquid flow. We applied our method for cavitating flows in a cascade. As a result of two-dimensional calculation, the quasi-steady and unsteady phenomena were reasonably simulated. The propagation of large-scale cavitation such as shedding of cloud cavitation was demonstrated. And we also report the results of three-dimensional calculation for unsteady cavitating flow in a pump inducer.

1 INTRODUCTION

In cavitating flows of turbomachines, instabilities as the cavitation surge and the rotating cavitation are observed. These instabilities have been studied experimentally[1] and theoretically[2]. The cavitating flow contains multi-scale unsteadiness, namely, from the dynamics of cavitation bubbles to the system instability in fluid machineries. Since the cavitation instabilities are very complex phenomena, numerical simulation might be suitable to obtain the detailed information about cavitating flow. The objective of the present study is to reproduce these unstable phenomena in cavitating flows by numerical simulation.

Since 1990's, various methods have been proposed to simulate cavitating flows as two-phase flows based on the Navier-Stokes equations. Kubota et al.[3], Schnerr & Sauer[4] and Tamura et al.[5] used the bubble dynamics model based on Rayleigh-Plesset equation. Reboud & Delannoy[6], Shin & Ikohagi[7], Qin et al.[8] and Dumont et al.[9] assumed barotopic fluid and used the equation of state for mixture of liquid and gas. Chen & Heister[10], Singhal et al.[11] and Kunz et al.[12] considered the mass transfer due to phase change at the surface of the liquid and vapor, and related proportionally between the rate of the phase change and the difference of local pressure and vapor pressure using empirical parameter. The empirical parameter is unknown, but this approach is quite simpler than the others.

Our method is based on the numerical method for incompressible fluid flow, but which has been employed the compressibility through the low Mach number as an assumption. The evolution of cavitation is determined by Chen & Heister cavitation model[10] with some modification considering the consistency with bubble dynamics[13]. This model is represented by the source/sink of vapor phase in the liquid flow.

One of us previously applied the present method for cavitating flows in a cascade[14]. As a result of two-dimensional calculation, the quasi-steady and unsteady phenomena were reasonably reproduced. But the cavitating flow calculated under multi passages condition was dominated not by the instability of cascade but rather by the cavitation instability itself. The rotating cavitation was not demonstrated clearly. The reason of this is considered due to the small solidity ($C/h = 0.81$) of cascade which is the same condition with the experiment[15]. It was reported by a theoretical analysis[16] that alternate blade cavitaiton is stable for a cascade with higher solidity ($C/h \geq 1.5$). So we calculated the cavitating flow in a cascade with the large solidity ($C/h = 1.62$) to reproduce the rotating cavitation.

In this paper, we report the results of two-dimensional calculation for the cavitating flow in a cascade of Clark Y-6% hydrofoil with the large solidity ($C/h = 1.62$). Firstly, assuming the 1-passage periodic condition, we mention about the steady and unsteady performance of cascade, such as the time-averaged lift coefficient, the strouhal number of lift fluctuation and pressure profile around the hydrofoil. Then, to consider the influence of interaction among cavitations in the passages, we calculate the cavitating flow under the 4-passages periodic condition. In ad-

dition, the numerical results of a fully three-dimensional simulation of unsteady cavitating flow through an axial pump with four blades are shown. Particular attention is focused for the three-dimensional structure of cavitation.

NOMENCLATURE

c speed of sound
C chord length of hydrofoil
C_L lift coefficient
C'_L lift coefficient fluctuation
C_l, C_g model constant for cavitation growth
f_G volumetric fraction of gas
f_L volumetric fraction of liquid
J metric Jacobian
M Mach number
p static pressure
p_v vapor pressure
p_∞ free-stream pressure
Re Reynolds number
u_i Cartesian velocity components
U^j contravariant velocity components
u_∞ velocity of uniform flow in far upstream
x_i Cartesian coordinates
σ cavitation number
ρ_L density of liquid
ν_L kinetic viscosity of liquid
ξ^j curvilinear coordinates
rms (sub) root-mean-square of fluctuation

(All variables are non-dimensionalized by C^*, u^*_∞ and the fluid density ρ^*_L, where subscript * means dimensional value.)

2 BASIC EQUATIONS

2.1 Governing Equations

In present study, all variables are non-dimensionalized by the fluid density ρ^*_L, the chord length of hydrofoil C^* and the velocity of uniform stream u^*_∞ respectively. Components of velocity vector are u_i in Cartesian coordinates x_i, and $U^j\,[=\beta^j_i u_i]$ in curvilinear coordinates ξ^j ($\beta^j_i = \partial\xi^j/\partial x_i$). The Jacobian of coordinate transform is $J\,(=|\partial x_i/\partial\xi^j|)$.

The volumetric fraction of liquid is f_L, the density of liquid and gas phase are ρ_L and ρ_G respectively. Assuming $\rho_G \ll \rho_L$ on $\rho = \rho_L f_L + \rho_G(1-f_L)$, a small density fluctuation ($\rho_L = 1+\rho'_L$, $\rho'_L \ll 1$) and an isentropic process ($D\rho'_L/Dt = M^2 Dp/Dt$), the mass conservation equation is represented as

$$\frac{Df_L}{Dt} + f_L\left[M^2\frac{Dp}{Dt} + \frac{1}{J}\frac{\partial(JU)^j}{\partial\xi^j}\right] = 0, \tag{1}$$

where p is the static pressure. The Mach number $M\,(=u_\infty/c)$ is given uniformly in a computational domain.

The equation of momentum is formulated as

$$\frac{\partial u_i}{\partial t} + U^j\frac{\partial u_i}{\partial\xi^j} = -\frac{1}{f_L}\beta^k_i\frac{\partial p}{\partial\xi^k} + \frac{1}{J}\frac{\partial}{\partial\xi^k}\left(J\beta^k_j\tau_{ij}\right), \tag{2}$$

in which τ_{ij} is the viscous stress components as

$$\tau_{ij} = \frac{1}{Re}\left(\beta^l_j\frac{\partial u_i}{\partial\xi^l} + \beta^m_i\frac{\partial u_j}{\partial\xi^m} - \frac{2}{3}\delta_{ij}\frac{1}{J}\frac{\partial JU^n}{\partial\xi^n}\right), \tag{3}$$

where $Re\,(=Cu_\infty/\nu_L)$ is Reynolds number with liquid kinetic viscosity ν_L. A turbulence model is not contained in the above equations since it has not been established for cavitating flows.

2.2 Cavitation Model

Chen & Heister[10] proposed a model to express cavitation growth and contraction by

$$\frac{D\rho}{Dt} = C(p-p_v), \tag{4}$$

where $C(=C_0L^*U^*>0)$ is an empirical constant and p_v is the vapor pressure. In the region $p<p_v$, Eq.(4) decreases the mixture density ρ in order to set the local pressure to the vapor pressure.

To modify Eq.(4), we considered the Rayleigh-Plesset equation as $DR/Dt = \sqrt{2(p_v-p)/3\rho_L}$, where viscous effects was ignored and pressure inside bubble was assumed to be the vapor pressure for $R \gg R_0$[17]. Using relation between void fraction f_G and bubble radius R under the constant bubble number density n, $Df_G/Dt = (36\pi n)^{1/3}{f_G}^{2/3}\sqrt{2(p_v-p)/3\rho_L}$ is derived, furthermore roughly approximation leads to a formula $Df_L/Dt = C(1-f_L)(p-p_v)$ with $f_L+f_G=1$. However, $f_L=1$ even if $p<p_v$ cavity doesn't grow, so we modify the model accordingly as

$$\frac{Df_L}{Dt} = \left[C_g(1-f_L) + C_l f_L\right](p-p_v) \tag{5}$$

to describe the onset of cavitation, where C_g and $C_l(=C_{l0}L^*U^*/\rho^*_L)$ are empirical constants. These values have not been experimentally or theoritically established. Thus, they are determined by the numerical optimization. In addition, p_v is given through the cavitation number, $\sigma = (p_\infty - p_v)/(\frac{1}{2}\rho_L u^2_\infty)$.

2.3 Boundary Conditions

Although the collapse of each bubble is not individually resolved, the high pressure fluctuation is caused by the collapse of the cloud cavitation. The pressure wave propagates to outfield of numerical domain, so particular attention has been paid to maintain the non-reflecting condition at the boundary. We used the boundary condition[13] avoiding the non-physical behavior when the strong pressure waves or vortices pass through to the open boundaries.

3 NUMERICAL SCHEME

The time marching scheme is based on the fractional step method for incompressible fluid flow using the collocated arrangement of variables in curvilinear coordinates[18]. The convection term in Eq.(2) is approximated by an upstream biased finite difference method[19]. The viscous term is approximated by the fourth-order central difference method. And the Adams-Bashforth explicit scheme of the second-order accuracy is used for convective and viscous terms. For the pressure coupling, the pressure gradient term in the equation of momentum is evaluated implicitly in time. The other spacial derivatives are approximated by second-order central difference method.

The equation for pressure is derived as,

$$\frac{Df_L}{Dt} + {f_L}^{(n)}\Big\{M^2\Big(\frac{3p^{(n+1)} - 4p^{(n)} + p^{(n-1)}}{2\Delta t} + U^{k(n)}\delta_k p^{(n+1)}\Big) + \frac{1}{J}\delta_k\widetilde{JU}^k - \frac{\Delta t}{J}\delta_k\Big(\frac{J\beta_j^k\beta_j^l}{{f_L}^{(n)}}\delta_l p^{(n+1)}\Big)\Big\} = 0, \quad (6)$$

where $\widetilde{JU}^k$ is transformed from the fractional step velocity, and n, Δt and δ_k are respectively the step number, time increment and the second-order central difference operator. Df_L/Dt is calculated as $({f_L}^* - {f_L}^{(n)})/\Delta t$, the intermediate value of fraction of liquid ${f_L}^*$ is expressed as follows.

The time marching for f_L is decomposed into two steps. Once, the liquid phase fraction is explicitly predicted as ${f_L}^P = {f_L}^{(n)} + \Delta t\{C_g(1 - {f_L}^{(n)}) + C_l {f_L}^{(n)}\}(p^{(n)} - p_v)$. If ${f_L}^P < 1$, ${f_L}^*$ is evaluated as

$${f_L}^* = {f_L}^{(n)} + \Delta t\{C_g(1 - {f_L}^{(n)}) + C_l {f_L}^{(n)}\}(p^{(n+1)} - p_v), \quad (7)$$

elsewhere ${f_L}^* = 1$. Approximating $Df_L/Dt = (f_L^* - f_L^{(n)})/\Delta t$ and then using Eq.(7), Eq.(6) can be solved for $p^{(n+1)}$ by a relaxation method under the above-mentioned boundary conditions. Then the convection is taken into account to finish the time development for ${f_L}^{(n+1)}$.

4 TWO-DIMENSIONAL CALCULATION FOR CAVITATING FLOW IN A CASCADE

4.1 Numerical setup

Flow in a cascade, which consists of the pitch-chord ratio $h/C = 0.6185$ (the solidity $C/h = 1.62$) and the stagger angle 64.27 deg, is considered. The Reynolds number is fixed as $Re(= Cu_\infty/\nu_L) = 5 \times 10^5$. The computational domain is shown in Fig.1. The length from inflow boundary to L.E. and from T.E. to outflow boundary are 5 chord length. The computational grid near the hydrofoil, which profile is Clark Y-6%, is shown in Fig.2. Using a body fitted H-type computational grid, the number of grid points are $N_\xi = 320$, $N_\eta = 120$. The number of grid and the minimum spacing of grid on the hydrofoil surface are 160 points (ξ-direction) and $\min(\Delta\xi) = 2.0 \times 10^{-4}$, $\min(\Delta\eta) = 4.0 \times 10^{-4}$. To make the maximum of C.F.L. number nearly equal 0.1, time increment is $\Delta t = 1 \times 10^{-5}$. We set temporary the model parameters as $C_g = 1000$, $C_l = 1$ if $p \le p_v$ and $C_g = 100$, $C_l = 1$ if $p > p_v$. Mach number is $M = 0.1$ uniformly, which manifests as weak compressible in our numerical setup : the time increment and the grid resolution. The periodic boundary condition is applied in the y-direction. The velocity of uniform flow is $|\boldsymbol{u}| = 1.0$ at inflow boundary and the static pressure of freestream is $p_\infty = 0.0$ at outflow boundary. We used non-cavitating flow data as the initial condition to calculate for the cavitating flow and took the average of flow data after the flow fully developed.

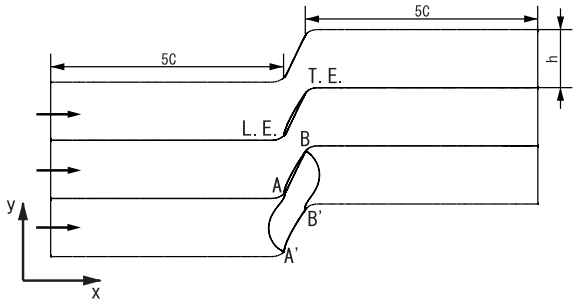

Figure 1. Computational domain for the calculation of flow around the cascade

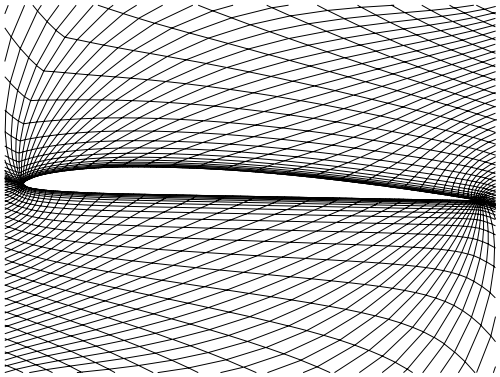

Figure 2. Computational grid near a hydrofoil (Clark Y-6%)

4.2 1-passage periodic condition

We calculated non-cavitating flow and compared the numerical result with experimental data[15] to check our scheme and grid resolution for computation. But there was no experimental data for the cascade with large solidity. So we compared the computational result with experimental data for small solidity case ($C/h = 0.81$), since we used the same computational code to calculate large solidity case ($C/h = 1.62$). Fig.3 compares the lift coefficient as a function of angle of attack with experimental data in non-cavitating flow condition. The result reasonably agrees with experimental data except as high α_∞. The reason of this discrepancy in higher α_∞ is considered due to the effect of turbulence, because we observed the separation region clearly in

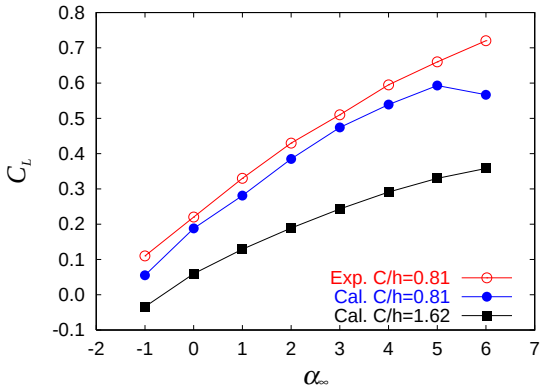

Figure 3. Lift coefficient as a function of angle of attack without cavitation (experimental data in Numachi et al.[15])

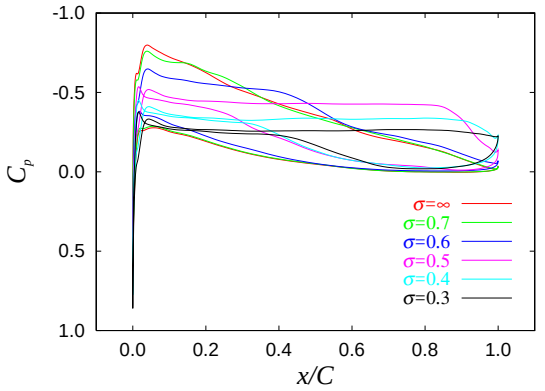

Figure 4. Profile of time-averaged pressure coefficient on the hydrofoil surface comparing for various cavitaion number ($C/h = 1.62$, $\alpha_\infty = 4\,\mathrm{deg}$)

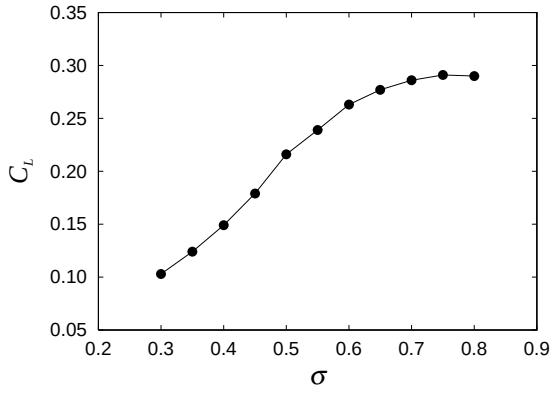

(a) Time-averaged lift coefficient

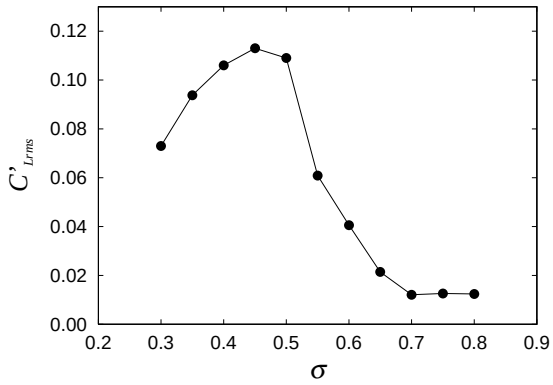

(b) Intensity of fluctuation of lift coefficient

Figure 5. Influence of cavitation number against performance of cascade (C/h=1.62, $\alpha_\infty = 4\,\mathrm{deg}$)

higher α_∞. But there was no separation region in high solidity case ($C/h = 1.62$), so we believe our simulation is sufficiently accurate.

Fig.4 compares profile of time-averaged pressure coefficient on the hydrofoil surface for various cavitation number under $\alpha_\infty = 4\,\mathrm{deg}$ condition. As cavitation number decreases, cavitation region is getting longer in where pressure coefficient is nearly equal to $-\sigma$. And in smaller cavitation number, cavitaiton was observed not only on suction side but also on pressure side near the leading edge. These cavitation had never been observed in smaller solidity case ($C/h = 0.81$)[14]. So it is considered that the interaction of cavitation among passages becomes strong.

Fig.5 shows time-averaged lift coefficient C_L and intensity of fluctuation of lift coefficient C'_{rms} as a function of cavitation number. C_L decreases gradually from $\sigma = 0.8$ to $\sigma = 0.6$, but C_L decreases linearly in smaller than $\sigma = 0.6$. As the suction side is covered with cavitation in smaller cavitaion number, pressure at the suction side increases linearly with decreasing cavitaion number (shown in Fig.4). On the other hand, C'_{rms} increases from $\sigma = 0.8$ to $\sigma = 0.45$. Especially C'_{rms} changes drastically between $\sigma = 0.6$ and $\sigma = 0.5$, when the cavitation develops to the trailing edge and the large scale cloud cavitaiton is produced. And C'_{rms} decreases in smaller cavitation number than $\sigma = 0.45$. The reason of this is considered that the attached sheet cavitation itself absorbs the change of the rate of flow owing to the growth/collapse of cloud cavitation.

Fig.6 compares spectrums of Strouhal number of lift coefficient fluctuation for various cavitation number. Strouhal number is getting smaller with decreasing cavitation number. But Strouhal number is constant $S_t \cong 0.24$ between $\sigma = 0.5$ and $\sigma = 0.4$, and intensity takes high value. It is because as the cavitation length becomes longer than the chord length, cloud cavitation is produced not by the flow turning around from over the sheet cavity to the cavity closure but by the flow turning around from suction side to the trailing edge. And when the sheet cavitation develops over the trailing edge, Strouhal number is getting smaller again. This feature of Strouhal number in the cavitaing flow around hydrofoil has been reported previously[20]. So we think both quasi-steady and unsteady cavitating flows were qualitatively reproduced by our calculation.

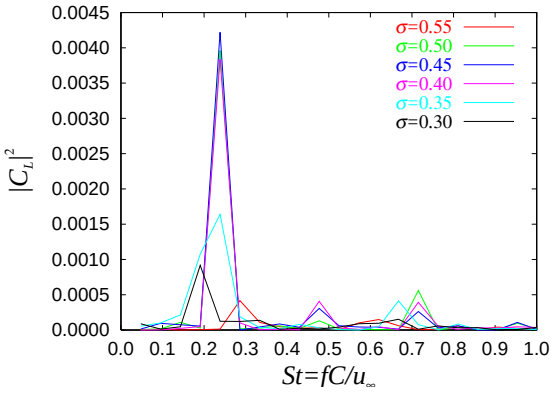

Figure 6. Spectrums of Strouhal number of lift coefficient fluctuation comparing for various cavitation number under 1-passage periodic condition

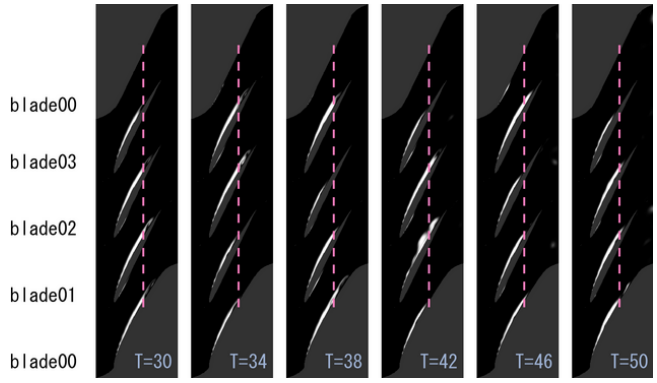

Figure 7. Instantaneous flow field represented by contour of liquid volumetric fraction

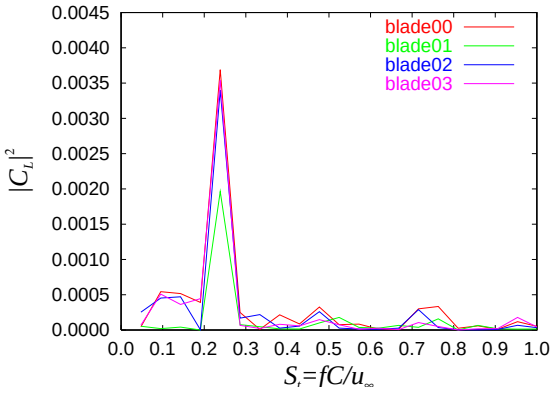

Figure 8. Spectrum of Strouhal number of lift coefficient fluctuation under 4-passage periodic condition ($\sigma = 0.5$)

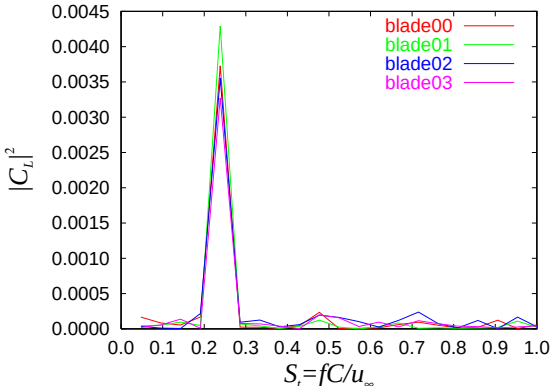

Figure 9. Spectrum of Strouhal number of lift coefficient fluctuation under 4-passage periodic condition ($\sigma = 0.4$)

4.3 4-passages periodic condition

We calculated the cavitating flow in a cascade assuming 4-passages periodic condition to reproduce the system instability. And we chose the cavitation number as $\sigma = 0.4$, 0.5 in which the intensity of fluctuation of lift coefficient was largest in our calculation (shown in Fig.5-(b)).

Fig.7 shows instantaneous flow field for cavity indicated by liquid volumetric fraction under $\alpha_\infty = 4\,\mathrm{deg}$ & $\sigma = 0.5$ condition, where time increment was chosen as $T = 4$ corresponding to $S_t \cong 0.24$. It is obviously shown that the sheet cavitation developing inhomogeneously among passages. This is because the change of flow rate through the passages owing to the growth or contraction of cavitation causes the instability of cascade. And it seems that the passage with the shorter sheet cavitaiton moves as blade No.3, 0&1, 2, 3&0, 2, 3. Fig.8 shows the spectrum of Strouhal number of lift coefficient fluctuation. Although the intensity of fluctuation is large at $S_t \cong 0.24$, the intensity of fluctuation in lower Strouhal number $S_t \cong 0.1 \sim 0.15$ becomes remarkably larger than the result of 1-passage periodic calculation shown in Fig.6. So the fluctuation of flow rate propagates in the period as $T \cong 7 \sim 10$.

Next, we calculated the cavitaing flow for smaller cavitation number $\sigma = 0.4$. The spectrum of Strouhal number of lift coefficient fluctuation is shown in Fig.9. In this case the sheet cavitations among passages were inhomogeneous at beginning of calculation, but gradually they became homogeneous. So the intensity of fluctuation is large at $S_t \cong 0.24$ only. We think the stable effect of cavitation is greater than the instability of cascade in smaller cavitation number.

5 THREE-DIMENSIONAL CALCULAITON FOR PUMP INDUCER

We calculated the cavitating flow in an axial pump like Fig.10, in which the blade is itself three-dimensional form. We added centrifugal force and Coriolis acceleration as

$$f_1 = 0,\ f_2 = x_2\omega^2 + 2u_3\omega,\ f_3 = x_3\omega^2 - 2u_2\omega \qquad (8)$$

into the right hand side of Eq.(2), where ω is the rotation velocity.

Numerical setup is as follows. The Reynolds number is fixed as $Re(= c_m r_b/\nu) \cong 4 \times 10^5$ and the rotation velocity is $\omega \cong 1.644$. Using a body fitted H-type computational grid, the number of

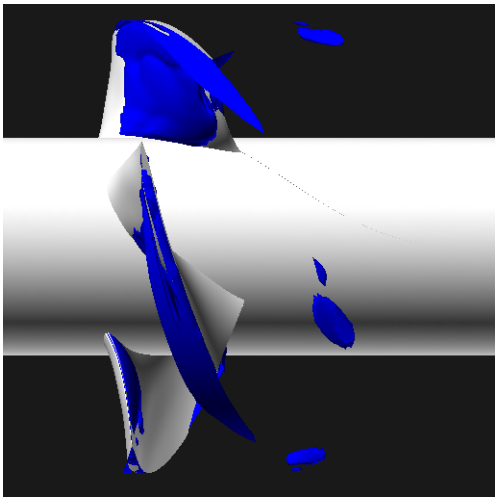

Figure 10. Instantaneous profiles of cavitation in an axial pump (indicated by $f_L = 0.9$ iso-surfaces)

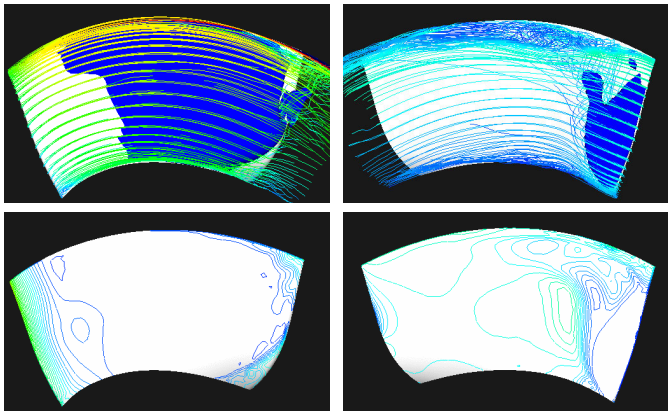

Suction side Pressure side

Figure 11. Instantaneous profiles of cavity indicated by $f_L = 0.9$ iso-surfaces, streamlines colored for $|\boldsymbol{u}|$ and pressure contours

grid points are $N_\xi = 240$, $N_\eta = 60$, $N_\zeta = 80$ in these directions, and 60×60 points on the blade surface. The periodic boundary condition was applied in the θ-direction, so only one passage was calculated. The cavitation number is $\sigma = 2.0$.

Fig.10 shows instantaneous flow field for cavity indicated by $f_L = 0.9$ iso-surface. And Fig.11 show stream lines near the surface and pressure contour on the surface. In the present numerical setting, sheet cavitation covered with pressure side as well as suction side of the blade. Consequently, the pressure is almost constant inside of attached sheet cavitation. We can also observe the cavitation which develops from tip to downstream. Although there is no tip clearance, it is caused by the interference between blade and casing. It should be note that the surface flow is turned in the direction of casing at cavity closure. To see the Fig.12, it is considered due to the pressure gradient at caivity closure. Hereby, not the production of the large scale cloud cavitation but the shedding a part of sheet cavitation was observed only.

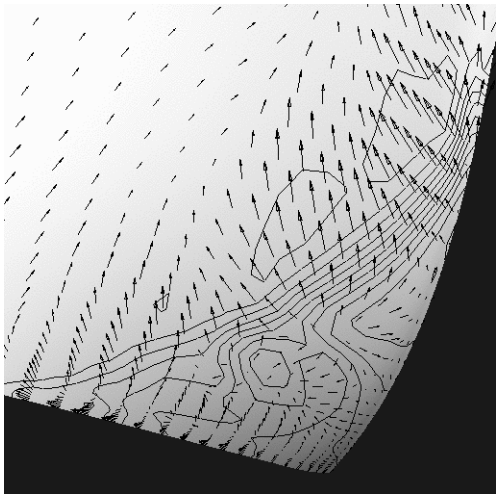

Figure 12. Close up view of the velocity vector on the surface of suction side near T.E.

6 CONCLUSION

To demonstrate the system instability, we calculated the unsteady cavitating flow in a cascade with large solidity ($C/h = 1.62$). And the numerical results of a fully three-dimensional simulation of unsteady cavitating flow through an axial pump with four blades were shown.

First, for 1-passage periodic condition, both quasi-steady and unsteady phenomena such as lift coefficient, pressure profile of hydrofoil and Strouhal number for various cavitation number were reasonably reproduced.

Next, we calculated the cavitating flow assuming 4-passages periodic condition. For lower cavitaion number case ($\sigma = 0.4$), the flow became homogeneous among passages because the stable effect of cavitation is greater than the instability of cascade. We could observe the system instability which was caused by growth and contraction of cloud cavitation under $\sigma = 0.5$ condition. And the frequency of this fluctuation is $S_t \cong 0.10 \sim 0.15$, that is lower than that of production of cloud cavitation as $S_t \cong 0.24$. But the mechanism of propagation in our calculation has been unknown, so we think it is needed to calculate the other condition furthermore.

Then, in three-dimensional calculation for cavitating flow in an axial pump, it was shown that the surface flow near the sheet cavitation was turned in the direction of casing by the pressure gradient generated at cavity closure. When the sheet cavitation develops three-dimensionally, the inverse flow at cavity closure is also highly three-dimensional. Hereby, it is decided whether the large scale cloud cavitaiton is produced or not.

Now we are trying to calculate the cavitating flow in the turbopump inducer shown in Fig.13, which is installed in the rocket engine. In the CAV2003, we might could show the numerical result.

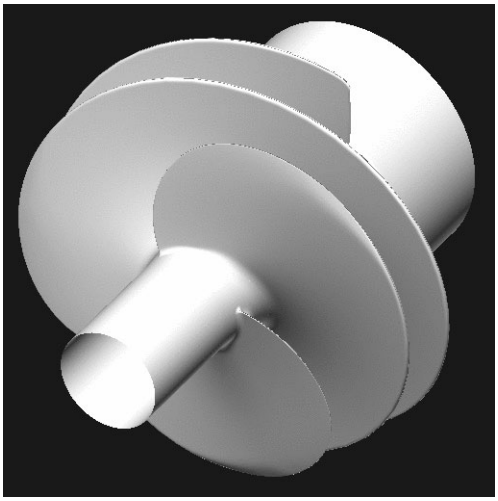

Figure 13. a turbopump inducer

REFERENCES

[1] Kamijo, K., Shimura, T. and Watanabe, M., 1980 "A Visual Observation of Cavitating Inducer Instability", *NAL Report*, TR-598T

[2] Tsujimoto, Y., Kamijo, K. and Brennen, C. E., 2001, "Unified Treatment of Flow Instabilities of Turbomachines", *Journal of Propulsion and Power*, Vol.17, No.3, pp.636-643

[3] Kubota, A., Kato, H. and Yamaguchi, H., 1992, "A New Modeling of Cavitating Flows - a Numerical Study of Unsteady Cavitation on a Hydrofoil Section", *J. Fluid. Mech.*, Vol.240, pp.59-96

[4] Schnerr, G. H. and Sauer, J., 2001, "Physical and Numerical Modeling of Unsteady Cavitation Dynamics", *4th International Conference on Multiphase Flow*, New Orleans

[5] Tamura, Y., Sugiyama, K. and Matsumoto, Y., 2001, "Physical modeling and solution algorithm for cavitating flow simulations", *15th AIAA Computational Fluid Dynamics Conference*, AIAA2001-2652

[6] Reboud, J. L. and Delannoy, Y., 1994, "Two-Phase Flow Modeling of Unsteady Cavitation", *The Second International Symposium on Cavitation*, pp.39-44

[7] Shin, B.-R. and Ikohagi, T., 1998, "A Numerical Study of Unsteady Cavitating Flows", *Third International Symposium on Cavitation*, pp.301-306

[8] Qin, J.-R., Yu, S.-T. J., Zhang, Z.-C. and Lai, M.-C., 2001, "Numerical simulation of transient external and internal cavitating flows using the space-time conservation element and solution element method", *Proc. ASME FEDSM'01*, New Orleans, CD-ROM FEDSM2001-18011

[9] Dumont, N., Simonin, O. and Habchi, C., 2001, "Numerical Simulation of Cavitating Flows in Diesel Injectors by a Homogeneous Equilibrium Modeling Approach", *4th International Symposium on Cavitation*, CAV2001:sessionB6.005

[10] Chen, Y. and Heister, S., 1995, "Two-Phase Modeling of Cavitated Flows", *Computer & Fluids*, Vol.24, No.7, pp.799-809

[11] Singhal, A. K., Baidya, N., and Leonard, A. D., 1997, "Multi-Dimensional Simulation of Cavitating Flows Using a PDF Model for Phase Change", *ASME Fluids Engineering Conference*, Vancouver, Canada

[12] Kunz, R. F., Boger, D. A., Stinebring, D. R., Chyczewski, T. S., Lindau, J. W., Gibeling, H. J., Venkateswaran, S., Govindan, T. R., 2000, "A preconditioned Navier-Stokes method for two-phase flows with application to cavitation prediction", *Computers & Fluids*, 29, pp.845-875

[13] Okita, K. and Kajishima, T., 2000, "Numerical investigation of unsteady cavitating flow around a rectangular prism", *Proc. 4th JSME-KSME Thermal Engineering Conference*, Kobe, Vol.2, pp.571-576

[14] Okita, K. and Kajishima. T., 2002, "Three-Dimensional Computation of Unsteady Cavitating Flow in a Cascade", *Proc. ISROMAC-9*, Honolulu, Hawaii, CD-ROM FD-076

[15] Numachi, F., Tsunoda, H. and Chida, I., 1949, *Rep. Inst. High Sp. Mech., Tohoku Univ.* Vol.1, No.5, pp.3-13 (in Japanese).

[16] Horiguchi, H., Watanabe, S., Tsujimoto, Y. and Aoki, M., 2000, "A Theoretical Analysis of Alternate Blade Cavitation in Inducers", *Trans. ASME, J. Fluids Eng.*, 122, pp.156-163

[17] Plesset, M. S. and Prosperetti, A., 1977, "Bubble Dynamics and Cavitation", *Ann. Rev. Fluid Mech.*, 9, pp.145-185

[18] Kajishima, T., Ota, T., Okazaki, K., and Miyake, Y., 1997, "High-Order Finite-Difference Method for Incompressible Flows using Collocated Grid System", *Trans JSME* Vol.63, No.614, Ser.B, pp.3247-3254 (in Japanese)

[19] Kajishima, T., 1994, "Upstream-shifted Interpolation Method for Numerical Simulation of Incompressible Flows", *Trans JSME* Vol.60, No.578, Ser.B, pp.3319-3326 (in Japanese)

[20] Arndt, R.E.A., Song, C.C.S., Kjeldsen, M., He, J., Keller, A., 2001, "Instability of Partial Cavitation : A Numerical/Experimental Approach", *Proc. of 23rd Symposium on Naval Hydrodynamics*, pp.599-615